Reprinted from Nuclear Instruments and Methods in Physics Research A 434 (1999) pp. 218-226.

ELSEVIER

Nuclear Instruments and Methods in Physics Research A 434 (1999) 218–226

NUCLEAR INSTRUMENTS & METHODS IN PHYSICS RESEARCH Section A

www.elsevier.nl/locate/nima

A silicon tracker for track extrapolation into nuclear emulsions

G. Catanesi[a], M. Contalbrigo[b], A. Cervera-Villanueva[c], A. De Santo[c], E. do Couto e Silva[c,*,1], D. Gibin[b], J.J. Gomez-Cadenas[c], W. Huta[c], J. Kokkonen[c], S. LaCaprara[b], B. Lisowski[d,2], M. Litmaath[c], E. Radicioni[a], S. Ricciardi[c], Ö. Runolfsson[c], S. Simone[a], U. Stiegler[c]

[a]*University of Bari and INFN, Bari, Italy*
[b]*University of Padova and INFN, Padova, Italy*
[c]*CERN, PPE Division, CH 1211 Geneva 23, Switzerland*
[d]*Dortmund University, Dortmund, Germany*

Received 2 March 1999; accepted 11 April 1999

Abstract

This paper describes the construction of a silicon tracker built to investigate how well silicon detectors can predict the position of particles in nuclear emulsions over a large area. The tracker consists of 72 single-sided silicon microstrip detectors with a total surface of 0.13 m^2 distributed over four layers, providing two x and two y coordinate measurements. The set-up was installed in a CERN PS pion beam in September 1997. © 1999 Elsevier Science B.V. All rights reserved.

Keywords: Silicon; Tracker; Emulsion

1. Introduction

At present, two experiments, CHORUS and NOMAD [1,2], are searching for $\nu_\mu(\nu_e) \leftrightarrow \nu_\tau$ oscillations in the CERN-SPS neutrino beam.

They are sensitive to small mixing angles in the limit of large mass squared difference. Experiments with a sensitivity at least an order of magnitude larger than CHORUS and NOMAD are being actively discussed [3–6]. These ν_τ appearance experiments are based on a target equipped with high-resolution tracking detectors, capable of detecting the topological signature of the τ decays.

Following the design of the TOSCA[3] experiment [7], we have built a set-up to investigate the possibility of combining silicon detectors and nuclear emulsions over a large area. The detector was installed in a CERN PS pion beam in September 1997. This exposure will measure the precision with which the silicon tracker can predict the position of particles in the emulsion.

* Corresponding author. Tel. +41-22-767-9229; fax +41-22-767-9070.

E-mail address: eduardo.do.couto.e.silva@cern.ch (E. do Couto e Silva)

[1] Now at Stanford Linear Accelerator Center, Stanford, CA, USA.

[2] On leave of absence from Institute of Electron Technology, Warsaw, Poland.

[3] Topological Oscillation Search with kinematical analysis.

0168-9002/99/$ - see front matter
PII: S0168-9002(99)00494-5

The organization of this paper is as follows. Section 2 describes the properties and the results of the tests of the silicon detectors. In Section 3 the ladder design is described and the results from ladder testing and noise studies are summarized. Section 4 describes the survey and its main results. The data acquisition system is described briefly in Section 5. Section 6 describes the offline alignment and some preliminary results. In Section 7 conclusions are presented.

2. Silicon tracker

The silicon tracker consists of 72 single-sided silicon microstrip detectors with an active surface of 0.13 m^2 distributed over four layers. It provides two x and two y coordinate measurements for each charged particle. A schematic drawing of these layers is displayed in Fig. 1.

The silicon detectors[4] are identical to those used in the DELPHI experiment [7]. These are single-sided, 33.5 mm × 59.9 mm, with strip and readout pitch of 25 and 50 μm, respectively. They are AC coupled, FOXFET biased [8] and passivated with silicon oxide. Each ladder is read out by five VA1 chips.[5] Each readout chip consists of 128 charge sensitive, low-power (1.2 mW/channel), low-noise preamplifiers followed by CR-RC shapers, sample-and-hold circuitry, output multiplexed and a multiplexed calibration circuit.

The mechanical frame to support the four layers is made of two half-pieces. As depicted in Fig. 2 each half-piece contains two silicon layers with strips oriented perpendicularly to each other. Each layer consists of six overlapping ladders and has an active area of about 18×18 cm^2. In order to minimize multiple scattering, ladders are made as thin as possible (see Section 3).

A custom-made water cooling unit[6] was used to compensate for the 30 W dissipated mainly by the readout electronics. This allowed to maintain a temperature stability of $22 \pm 1^{\circ}C$.

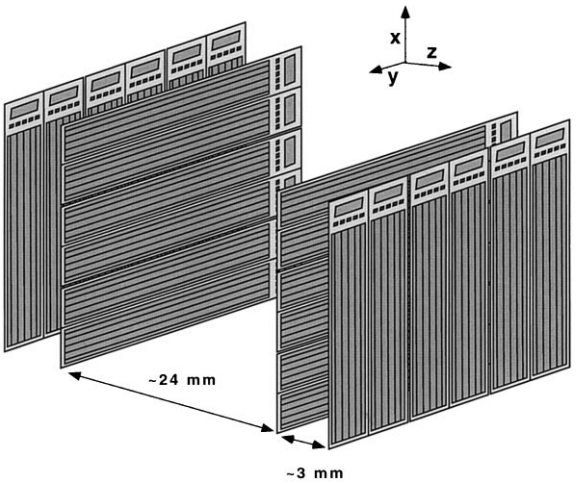

Fig. 1. Schematic drawing of the four silicon layers.

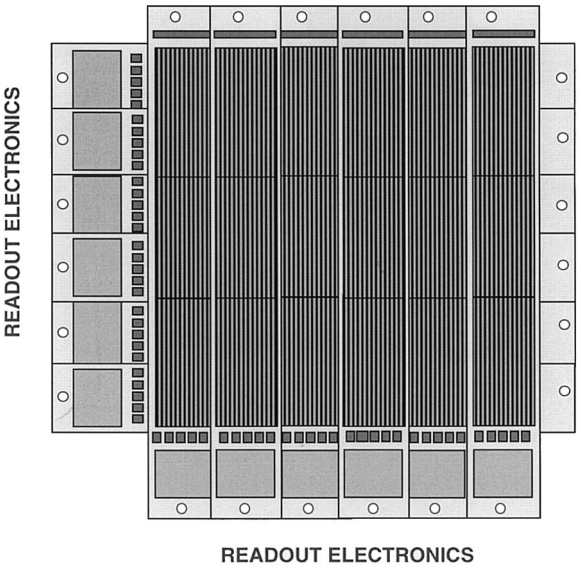

Fig. 2. Schematic drawing of a half-piece with two silicon layers.

2.1. Detector testing

The testing program has been fully described elsewhere [10].

A probe station with a high-magnification microscope and a CCD camera were used to

[4] Manufactured by Hamamatsu Photonics, Japan.

[5] A commercial version of the VIKING chip [9] manufactured by IDE AS, Norway.

[6] Manufactured at CERN.

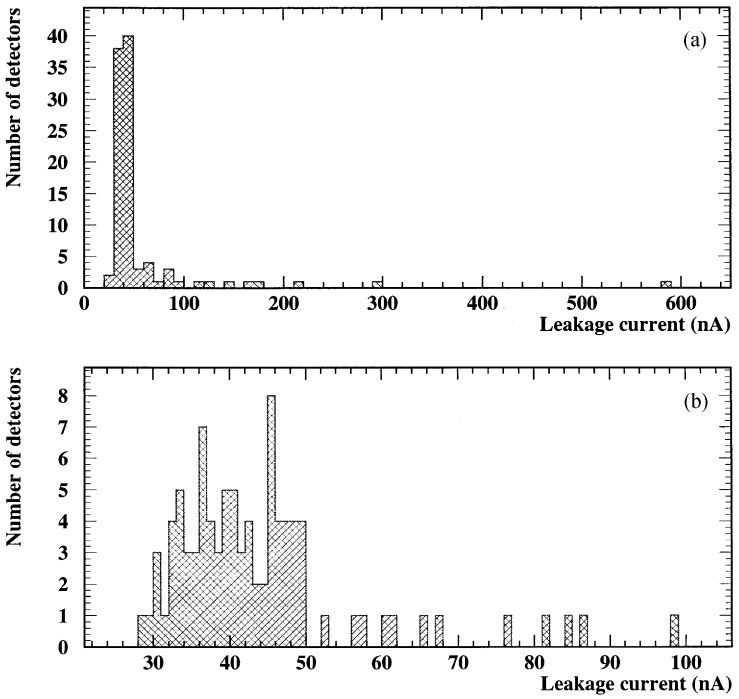

Fig. 3. Leakage current for: (a) all detectors and (b) detectors with leakage current smaller than 100 nA (92% of the total).

inspect the detectors. Only one detector had a processing error (seven interrupted floating strips) and was therefore rejected. Fig. 3a shows the measured leakage current for 100 detectors held at a bias voltage of about 70 V for about 24 h. In Fig. 3b only detectors with leakage current below 100 nA are displayed, corresponding to 92% of the total number of detectors.

3. Ladders

3.1. Ladder assembly

Fig. 4 illustrates the assembly of a ladder. Three silicon detectors are glued onto a common carbon fiber back bone (1 mm thick) and daisy-chained electrically using wire bonds. A thin glass epoxy foil is used to electrically isolate the detectors from the carbon fiber. Five VA1 chips are glued onto the glass epoxy foil and are wire bonded to a custom-made hybrid card.[7] A printed circuit made on the glass epoxy foil is used to connect the backplane of each detector to the bias line in the hybrid using 10 MΩ resistors. This printed circuit is also used to connect a capacitor to the backplane of the last detector in each ladder. A voltage step applied to this capacitor induces charge pulses in all strips for tests and calibration. At the far end of the foil, a metallized area serves as a ground plate. One of the main advantages of this design is the possibility of measuring directly on the hybrid, the leakage current for each detector separately.

This printed circuit foil improves the design described in Ref. [11]. It facilitates ladder debugging and reduces the number of gluing steps during ladder assembly.

The hybrid consists of a multilayer printed circuit board which contains a connector and surface

[7] Manufactured at CERN.

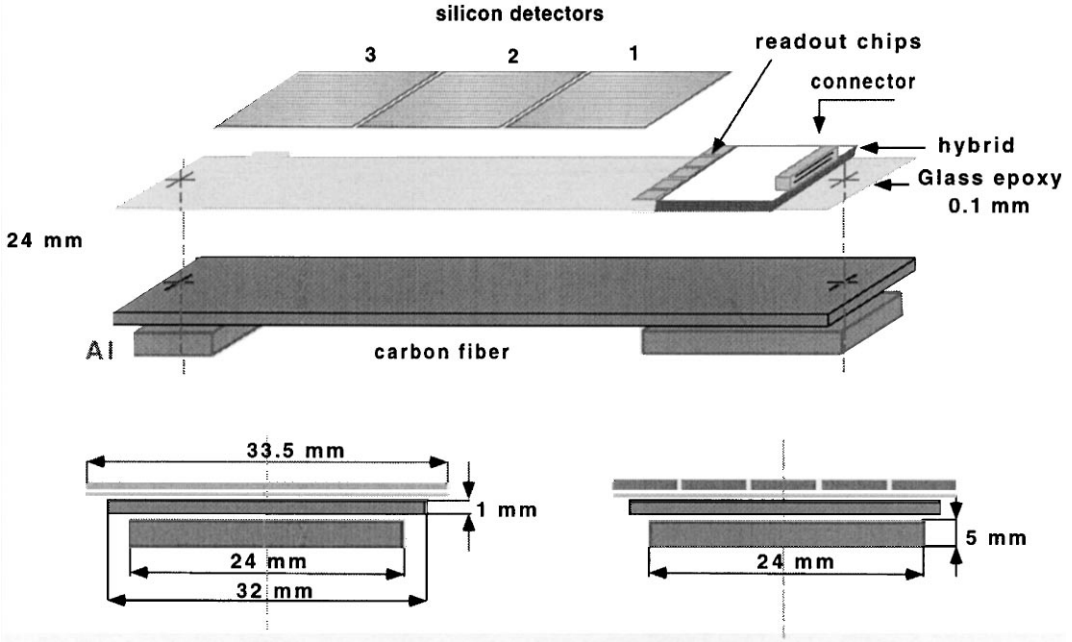

Fig. 4. Schematic drawing of a ladder.

mounted devices (SMD). It also improves the previous design [11]. For the hybrid used in Ref. [11], the test pulse calibration lines were too close to those that carry the analog output signals. This has been modified together with a better decoupling of the power lines, thereby reducing the impedance of power lines and minimizing cross-talk effects. As shown in the results given in Section 3.3, the better layout for the hybrid reduces the total noise in the system.

3.2. Ladder tests

The testing program for the ladders follow that of Ref. [11]: measurements of noise, leakage current and backplane pulsing. Each ladder was operated with a reverse bias voltage of 60 V with drain and FOXFET gate grounded. The signal-to-noise ratio was measured using a radioactive ruthenium source.[8] The results for all ladders are shown in Fig. 5. The signal-to-noise ratio was defined as the fitted peak position when a Landau distribution convolved with a Gaussian was used to fit the charge distribution for the cluster.

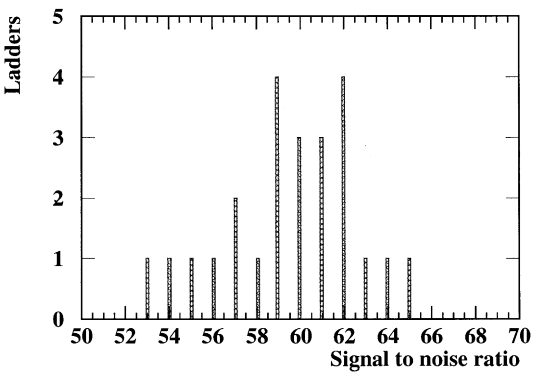

Fig. 5. Signal-to-noise distribution from laboratory measurements for 24 ladders.

The summary of the ladder tests after assembly is presented in Figs. 6a and b. In average a ladder had a leakage current of 150 nA and 0.2% defective channels.

[8] Electrons emitted with maximum energy of about 3.5 MeV.

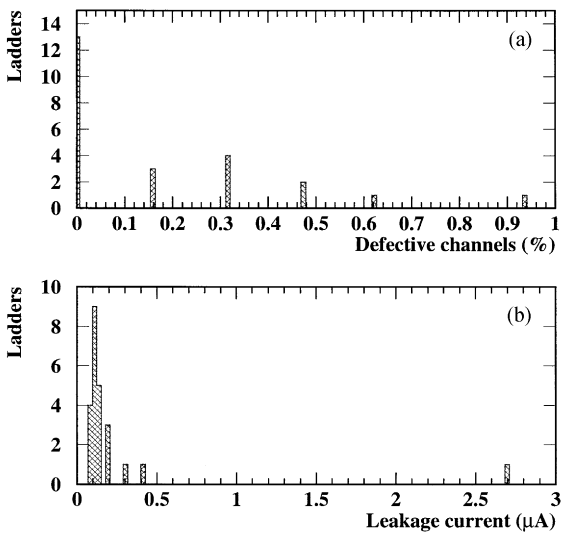

Fig. 6. (a) Percentage of defective channels for all ladders, (b) leakage current for all ladders.

3.3. Noise studies

To estimate the expected signal-to-noise ratio we use the mathematical model described in Ref. [11]. The total noise of a typical ladder, $\mathrm{ENC_{ladder}}$, is obtained by adding the sources of noise in quadrature

$$\mathrm{ENC_{ladder}} = \mathrm{ENC_{VA1}} \oplus \mathrm{ENC_{leak}} \oplus \mathrm{ENC_{res}} \oplus \mathrm{ENC_{ms}} \quad (1)$$

where ENC is the Equivalent Noise Charge which relates the root mean squared (rms) noise voltage at the output of the shaper directly to the signal strength at the input. $\mathrm{ENC_{VA1}}$ is the noise from the readout chip, $\mathrm{ENC_{leak}}$ is the noise from the leakage current, $\mathrm{ENC_{res}}$ is the noise from the biasing resistors and $\mathrm{ENC_{ms}}$ is the noise from the resistances of the metallization on the top of the strips and metallic conductors to the amplifier.

The parametrization for $\mathrm{ENC_{VA1}}$ was given in Ref. [11]:

$$\mathrm{ENC_{VA1}} = 169\mathrm{e}^- + 5.6\mathrm{e}^- C_\mathrm{t}\ (\mathrm{pF}) \quad (2)$$

where C_t is given in units of picofarads. In this model we assume that a minimum ionizing particle creates 25 000 electron–hole pairs when traversing $\simeq 300\,\mu\mathrm{m}$ of silicon.

The parameters contributing to the noise of a ladder have been measured in Ref. [11] and are listed in Table 1. The calculated value for the strip resistance takes into account the reduction in the equivalent series resistance as explained in Ref. [12]. The total parallel resistance (R_p) is obtained by

$$\frac{1}{R_\mathrm{p}} = \frac{N}{R_\mathrm{pol}} + \frac{1}{R_\mathrm{f}} \quad (3)$$

where N is the number of detectors in a ladder, R_pol is the dynamical resistance of the FOXFET for

Table 1
Summary of the parameters used in the model

Parameter	Measured value for a detector	Calculated value for a ladder
Interstrip capacitance	1.2 pF/cm	21.6 pF
Backplane capacitance	0.15 pF/cm	2.7 pF
Total capacitance (C_t)	1.35 pF/cm	24.3 pF
Strip resistance (R_ms)	31.5 Ω/cm	189 Ω
Leakage current per strip (I_leak)	0.04 nA	0.12 nA
FOXFET dynamical resistance	500 MΩ	–
Total parallel resistance (R_p)	–	62.5 MΩ

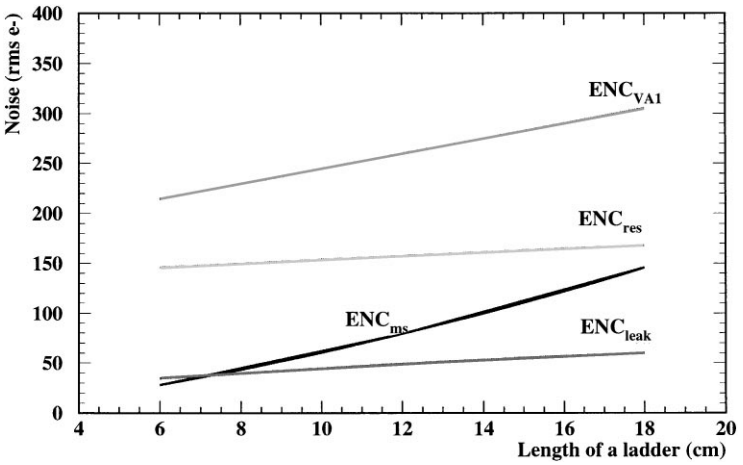

Fig. 7. Sources of noise versus the length of a ladder from theoretical predictions.

each detector and R_f is the feedback resistor of the preamplifier.[9]

Fig. 7 shows that the dominant noise contribution comes from the load capacitance at the input of the amplifier (ENC_{VA1}).

Predictions of the model and measurements performed using the radioactive source were compared. The signal-to-noise ratio was measured for a ladder with 1, 2 and 3 detectors (a detector has a length of 6 cm), respectively. The results are displayed in Fig. 8, where laboratory measurements are represented by the closed circles. The solid curve shows the calculated signal-to-noise ratio for a ladder versus its length which is in a good agreement with the data. For completeness, we display in Fig. 8 the measured data from Ref. [11] with the old hybrid design (open circles). The improved hybrid design results in a reduction of the total noise.

4. Survey

In order to achieve a spatial resolution of less than 10 μm, each layer had to be surveyed accurately. The survey equipment has a resolution of $\sigma_x \sim 6\,\mu m$, $\sigma_y \sim 6\,\mu m$ and $\sigma_z \sim 14\,\mu m$. A full description can be found elsewhere [10].

Initially, the two half-pieces that constitute the support frame were assembled without the ladders. Since the half-pieces are mounted back-to-back, the frame must be rotated so that both sides can be surveyed. Precision marks were used to establish the systematic uncertainties due to this rotation. After that, 12 ladders were mounted on a half-piece to be surveyed. Finally, the 12 remaining ladders were mounted on the second half-piece and both pieces were joined together to be surveyed. The resolution in both X and Y were determined from the measurement of the strip length of each detector. As shown in Fig. 9, these are better than 5 μm. The improvement seen with respect to the results presented in Ref. [10] is ascribed to a better calibration of the survey equipment. Here the angle between the X and Y axis was taken to be different from 90°. To speed up the scanning time during the survey the requirement on the resolution for the Z coordinate was relaxed to be better than 50 μm. The systematical uncertainties due to the mounting and dismounting of the ladders and the rotations of the frame have been estimated to be better than 20 μm.

[9] It is expected to be at least 50 MΩ [9]; in our calculations we assumed $R_f = 100$ MΩ.

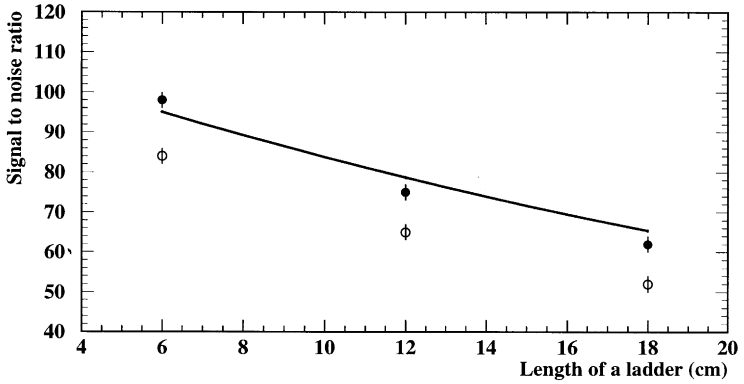

Fig. 8. Calculated signal-to-noise ratio (solid curve) versus the length of the ladder. The laboratory measurements with the new (old) hybrid design are represented by the closed circles (open). The error bars quoted represent estimated uncertainties of the measurement procedure.

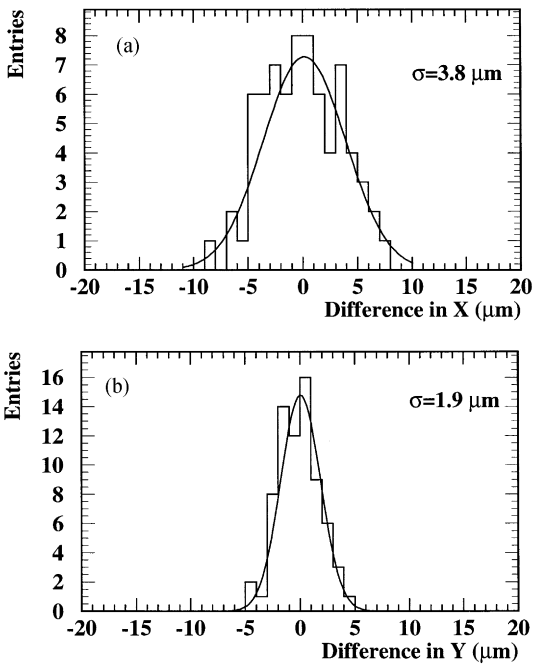

Fig. 9. Resolution of the surveying system. Systematic differences in the measurements of the coordinates (a) X and (b) Y.

5. Data acquisition

The signal coming from a readout strip is fed into a VA1 preamplifier [9]. Each VA1 chip has 128 input channels and one single multiplexed output. Each ladder contains five readout chips, which are wire bonded to the strips. The VA1 chips are daisy-chained in groups of 10; in this way signals coming from two ladders are sequentially read out through an interface card (repeater card). On the repeater signals are further amplified and sent through a 30-m long twisted pair cable to a single ADC. In this configuration, 12 ADCs connected in parallel read out the entire detector (15 360 channels). We used 6 dual 10-bit flash ADC CAEN V550 VME modules operated at 1 MHz conversion frequency. The total conversion and storage time to the on-board FIFO was approximately 1.3 ms. The VA1 and V550 operations were synchronized by a CAEN V551 sequencer. After a trigger signal, the sequencer provides a hold signal to the VA1 readout chips and then sends multiplexing signals to the VA1s and conversion clocks to the ADCs. All the control and multiplexing signals to the VA1s are also routed by the repeater card. The ADC FIFOs were read out by an FIC8234 processor and sent to a UNIX front-end workstation, where run control and monitoring were performed to provide online displays of pedestals, noise and common mode shift for each readout chip.

6. Alignment

To optimize the precision of the track extrapolation from the silicon tracker to the emulsion target,

the layers of silicon detectors are aligned using particle tracks. Having only two layers for each projection in the transverse plane, the geometry of the modules has to be exploited, selecting particles going through the overlap region between adjacent ladders. Alignment runs, with the magnetic field switched off, have been recorded in correspondence to each physics measurement, without changing the experimental conditions.

The clusterization algorithm searches for a strip with local maxima in the signal-to-noise variable (seed strip). For the seed strip with a signal above a fixed threshold, a cluster is formed with up to three adjacent strips included per side. Signal sharing between adjacent clusters using the same strip is allowed. To avoid any ambiguity, single track events have been selected, with only one hit in the overlap region in each of the four considered ladders. Only relative displacements perpendicular to the z direction (see Fig. 10) have been taken into account, while rotation effects have been considered as second-order corrections and therefore neglected.

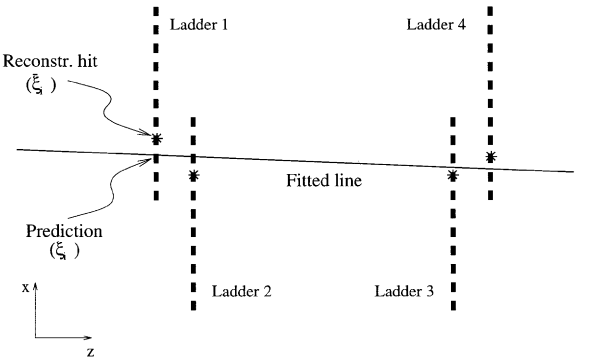

Fig. 10. Schematic drawing of the silicon detector. Only the planes in one projection are shown and particularly the overlapping ladders where the beam impinges.

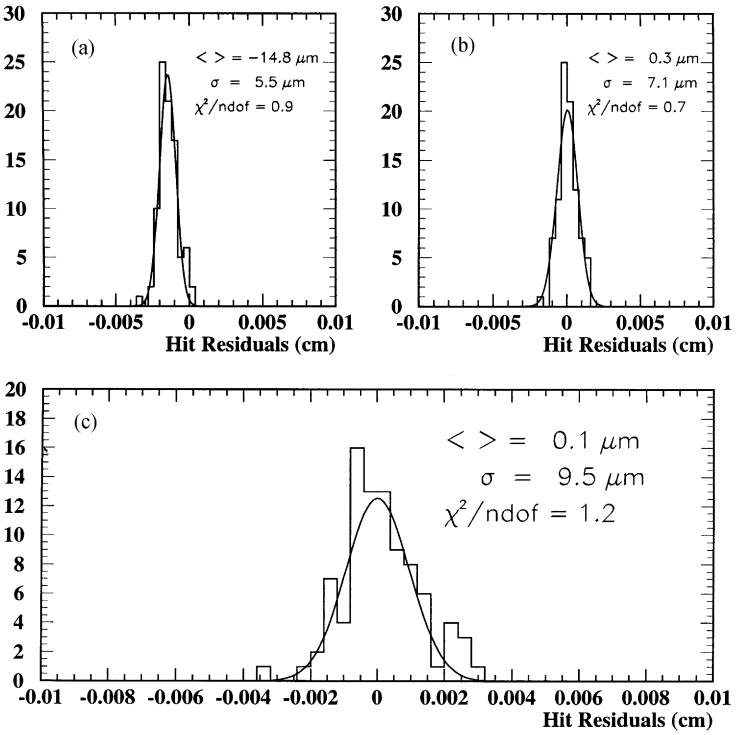

Fig. 11. Hit residuals on the first central ladder along the bending direction: (a) before and (b) after the alignment, using the 4-hit linear fit for the prediction, and (c) after the alignment using the 3-hit fit. The solid curves correspond to Gaussian fits to the distributions.

As shown in Fig. 10 the transverse coordinates of the four hits ($\bar{\xi}_i$, $i = 1, \ldots, 4$) are used to perform a linear fit and, once the straight-line parameters have been extracted, one predicts the particle intercept on each ladder (ξ_i, $i = 1, \ldots, 4$). Since tracks are almost perpendicular to the detector planes, the errors on the longitudinal position are ignored. For each hit a "residual" (Δ_i) is defined as

$$\Delta_i \equiv \bar{\xi}_i - \xi_i, \quad i = 1, \ldots, 4. \tag{4}$$

This quantity is normally distributed and the mean value of the Gaussian represents the shift of the considered ladder with respect to its nominal position.

Figs. 11a and b show the hit residuals for the first ladder whose measured coordinate lies along the bending projection, before and after the alignment, respectively. The result of the Gaussian fit is also given: the ladder, which was shifted by $\approx 15\,\mu m$ with respect to the nominal position, can be realigned to better than $1\,\mu m$.

This $15\,\mu m$ offset is in good agreement with the systematical uncertainties described in Section 4.

After the positions of the four ladders have been corrected, a linear fit is performed including only three points in the χ^2, and the hit residuals on the excluded layer are calculated. As depicted in Fig. 11c, the width of the distribution is of the order of $10\,\mu m$, which is consistent with the intrinsic resolution of the silicon detector [11].

7. Conclusion

We have described the construction of a silicon tracker that will be used to verify how accurately microstrip detectors can predict the position of particles in nuclear emulsions over a large area.

This tracker was built with a detector yield of 99%. A typical ladder has an average signal-to-noise ratio of 60, 0.2% defective channels and a leakage current of about 150 nA. Our predictions for the signal-to-noise ratio agree very well with the measured data. Ladders were assembled in a frame and surveyed to a precision better than $20\,\mu m$. Preliminary results from the data indicate that the tracker is aligned to the predicted mechanical precision.

Acknowledgements

Special thanks to G. Gregoire, L. Camilleri, L. Linssen and J. Panman for fruitful discussions and comments to this manuscript. We also acknowledge the help from I.M. Papadopoulos. We are indebted to the OPAL and CMS groups for providing an incredible support including the laboratory infrastructure. Thanks to Kasper "always ready to bond" Mühleman, R. Dumps, J. Mulon, L. Liberti, G. Barichello and C. Rosset. Last but not least thanks to the support of the TOSCA institutes and especially those who worked in the preparations for the test beam set-up.

References

[1] E. Eskut et al., CHORUS Collaboration, Nucl. Instr. and Meth. A 401 (1997) 7.
[2] J. Altegoer et al., NOMAD Collaboration, Nucl. Instr. and Meth. A 404 (1998) 96.
[3] J.J. Gomez-Cadenas, J.A. Hernando, A. Bueno, Nucl. Instr. and Meth. A 378 (1996) 196.
[4] J.J. Gomez-Cadenas, J.A. Hernando, Nucl. Instr. and Meth. A 381 (1996) 223.
[5] A. Ereditato, P. Strolin, G. Romano, Nucl. Phys. Proc. Suppl. B 54 (1997) 139.
[6] A.S. Ayan et al., A high sensitivity short baseline experiment to search for $\nu_\mu \leftrightarrow \nu_\tau$ oscillation, CERN-SPSC/97-5, SPSC/I213, March 1997.
[7] P. Chochula et al., Nucl. Instr. and Meth. A 412 (1998) 304.
[8] P.P. Allport et al., Nucl. Instr. and Meth. A 310 (1991) 155.
[9] O. Toker et al., Nucl. Instr. and Meth. A 340 (1994) 572.
[10] G. Barichello et al., Nucl. Instr. and Meth. A 419 (1998) 1.
[11] G. Barichello et al., Nucl. Instr. and Meth. A 413 (1998) 17.
[12] I. Kipnis, Noise analysis due to strip resistance in the ATLAS SCT silicon strip module, LBL Internal Report, LBNL-39307, August 1996.